Composite Structures 214 (2019) 293–303

Contents lists available at ScienceDirect

Composite Structures

journal homepage: www.elsevier.com/locate/compstruct

Anisotropy compensated MUSIC algorithm based composite structure damage imaging method

Qiao Bao, Shenfang Yuan*, Yanwen Wang, Lei Qiu

Research Center of Structural Health Monitoring and Prognosis, The State Key Lab of Mechanics and Control of Mechanical Structures, Nanjing University of Aeronautics and Astronautics, 29 Yudao Street, Nanjing 210016, People's Republic of China

ARTICLE INFO

Keywords:
Synthesis aperture-MUSIC
Damage localization
Anisotropy compensation
Phase errors estimation
Reinforced composite structure

ABSTRACT

Multiple signal classification (MUSIC) algorithm is a promising method in guided wave based structural health monitoring (SHM) area because of its directional scanning ability and easy arrangement of the sensor array. However, since composite structures are anisotropic, guided waves have different velocities along different directions, i.e. propagation anisotropy. For different scanning positions of the monitoring area in MUSIC algorithm, the directions from the scanning position to the sensor array are different. Even for the same scanning position, the directions from the scanning position to each element in the sensor array are also different. If a fixed velocity is used in MUSIC algorithm, there must exist sensor phase errors in steering vectors of MUSIC algorithm caused by structural anisotropy, as well as the sensor position error, resulting in the localization error. To reduce the localization error caused by sensor phase errors, an anisotropy compensated MUSIC algorithm is proposed, which could compensate different kinds of sensor phase errors jointly and improve the localization precision and reliability of MUSIC algorithm. The proposed method is verified on a reinforced composite panel with one T-stiffener. Experimental results show that the proposed method can realize damage localization with an obviously improved accuracy.

1. Introduction

Due to their superior characteristics, the application of composite materials in modern aircraft structures has grown steadily [1,2]. However, composite structures are susceptible to internal damage caused by low-velocity impact during the manufacture and service. Damage monitoring of composite structures has been an important task of structural health monitoring (SHM), which can ensure the safety and reduce the maintenance cost of aircrafts [3–5]. Among SHM methods, since guided wave based SHM method is sensitive to small damage and could realize large area monitoring, it has been considered as a promising technique for online monitoring of aircraft structures [6–9].

Traditional Lamb wave based SHM methods usually use the sparse sensor layout, which is difficult to be arranged on aircraft structures. In recent years, compact sensor array based multiple signal classification (MUSIC) algorithm was introduced to guided wave based SHM method, which has directional scanning ability and the potential to monitor multiple sources [10,11]. So far, most research of MUSIC algorithm based SHM methods are focused on impact localization [12–17]. The research of MUSIC algorithm based damage localization is still lack. A linear sensor array based near-field MUSIC algorithm was proposed by Zhong and Yuan for detecting damage on a carbon fiber composite material plate [18]. Even the research was verified on a composite structure, the structural anisotropy was not considered. Suffering from the low signal to noise ratio (SNR) of damage scattered signal caused by high attenuation of guided wave, the MUSIC algorithm based damage localization method usually fails. For this problem, Bao and Yuan proposed a transmitter beamforming and weighted image fusion based MUSIC algorithm, which realized corrosion damage monitoring [19]. However, this method is just verified on a simple aluminum plate. Different from impact localization, an active guided wave based SHM method is needed for damage monitoring. Thus, the complicated propagation properties of guided wave on aircraft composite structures have an impact on the performance of MUSIC algorithm. To monitor damage on composite structures using the MUSIC algorithm, some issues remain open. Firstly, because of the anisotropy of composite materials, the propagation velocities of guided wave along different directions are also different [20]. For different scanning positions of the monitoring area in MUSIC algorithm, the directions from the scanning position to the sensor array is different. Even for the same scanning position, the directions from the scanning position to each element in the sensor array are also different. If a same velocity is used in the

* Corresponding author.
E-mail address: ysf@nuaa.edu.cn (S. Yuan).

https://doi.org/10.1016/j.compstruct.2019.02.036
Received 6 August 2018; Received in revised form 2 January 2019; Accepted 8 February 2019
Available online 10 February 2019

scanning process of MUSIC algorithm, it would lead to the error of time delay estimation from the damage to every element of the sensor array, which is known as the sensor phase error [21,22]. Also, in practical applications, the sensor position error is inevitable when bonding the sensor array on structures, which leads to the phase error too [23]. The sensor phase errors would influence the orthogonality between steering vectors and the noise subspace, which results in localization error. Secondly, due to the high attenuation of guided wave on composite structures, the transmitter beamforming based MUSIC algorithm is needed to improve the SNR of damage scattered array signals in the previous research. But the sensor phase errors also exist during the excitation process. In this case, the performance of transmitter beamforming would both degrade [24].

To deal with these problems, an anisotropy compensated MUSIC algorithm, i.e. synthesis aperture-MUSIC algorithm with sensor phase errors estimation, is proposed to localize damage on reinforced composite structures. In this paper, the sensor phase errors caused by the structural anisotropy and sensor position error are quantitatively analyzed firstly, as well as the influence of these errors on the performance of synthesis aperture signal processing and MUSIC algorithm. Based on this research, an omnidirectional sensor phase errors estimation method is proposed. With sensor phase errors compensation, the performance of synthesis aperture signal processing could be improved and the steering vectors in MUSIC algorithm could be calibrated, which makes MUSIC algorithm more precise and reliable for damage localization on composite structures. To verify the proposed method, an experiment of damage localization on a reinforced composite plate with one T-stiffener is performed. Experimental results show that this method successfully localizes the damage on reinforced composite structures.

This paper is organized as follows: Section 2 introduces the basic principle of synthesis aperture-MUSIC algorithm for damage localization. Then the guided wave performance on a reinforced composite panel is researched in Section 3. In Section 4, the time delay error of the linear array and its influence on the performance of synthesis aperture signal processing and MUSIC algorithm are quantitatively analyzed. And the synthesis aperture-MUSIC algorithm with sensor phase error estimation for damage localization on composite structures is proposed. In Section 5, the damage localization experiment is performed on a reinforced composite panel and the details of damage localization are depicted. Eventually, Section 6 gives the conclusion.

2. Synthesis aperture-MUSIC algorithm for damage localization

Firstly, on the basis of transmitter beamforming and MUSIC algorithm, a synthesis aperture-MUSIC algorithm using a dual array is briefly introduced [19]. This method employs a dual array, consisting of two linear sensor arrays. Then the method generates the guided wave through actuating one sensor array and receives the guided wave with another sensor array. Then in one search step of monitoring area, the focused signal is attained through making the guided wave actuated from every element in the actuator array to arrive at the damage simultaneously. With this focused array signal, the noise subspace and steering vectors are calculated based on MUSIC algorithm, as well as the spatial spectrum to describe the orthogonality between them. As the monitoring area is overall searched, the synthesis aperture and spatial spectrum calculation can be attained through only one search, which is the synthesis aperture-MUSIC algorithm.

As seen in Fig. 1, a dual array consisting of two linear sensor arrays is arranged on the structure, including array A and array S. Each linear sensor array has $2M + 1$ elements with a spacing of d. The distance between two linear sensor arrays is l. $\boldsymbol{A}(r,\theta)$ is defined as the array steering vector.

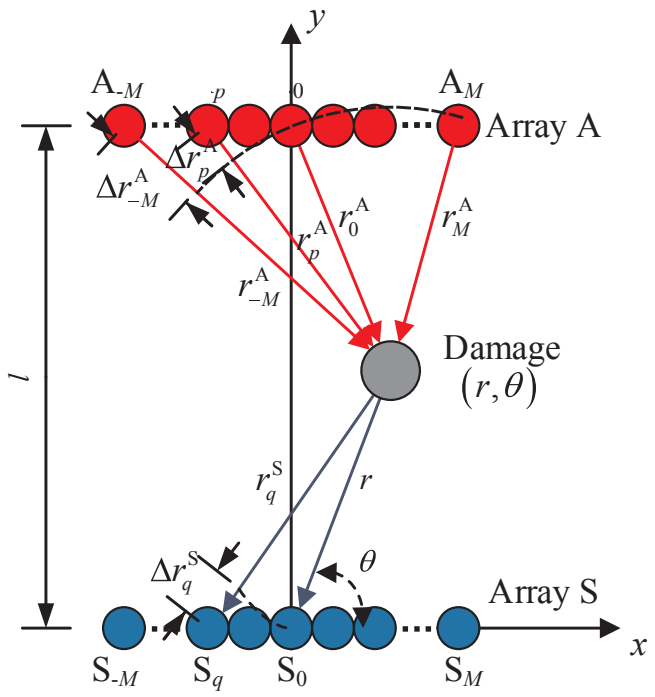

Fig. 1. Schematic diagram of synthesis aperture-MUSIC algorithm using a dual array.

$$A(r,\theta) = [a_{-M}(r,\theta) \quad a_{-M}(r,\theta) \quad a_{-M+1}(r,\theta) \quad \cdots \quad a_M(r,\theta)]$$
$$a_q(r,\theta) = e^{j\omega_0\tau_q},\ q = -M,\cdots M$$
$$\tau_q = \frac{\Delta r_q^S}{c} = \frac{r - r_q^S}{c} = \frac{r - \sqrt{r^2 + q^2d^2 - 2rqd\cos\theta}}{c} \tag{1}$$

r is defined as the distance between the damage and the reference element, which is PZT S_0 here. θ denotes the wave propagation direction corresponding to the x-axis. τ_q is the relative time delay from damage to PZT S_q corresponding to the reference element. r_q^S denotes the distance between the damage and PZT S_q. c is the propagation velocity of the guided wave with the center frequency of ω_0.

Assuming array A is the actuator array to generate guided wave and array S is then used to receive the scattering wave from the corrosion, the scattered array signals from the damage can be acquired, which are denoted as $\boldsymbol{X}_{-M}(t)$, $\cdots$,$\boldsymbol{X}_M(t)$. The subscript represents the element in the actuator array. Then the focused scattered array signals are calculated [19],

$$\boldsymbol{X}(t) = \boldsymbol{X}_{-M}(t)\cdot e^{-j\omega_0 t_{-M}} + \cdots + \boldsymbol{X}_p(t)\cdot e^{-j\omega_0 t_p} + \cdots + \boldsymbol{X}_M(t)\cdot e^{-j\omega_0 t_M},$$
$$p = -M,\cdots M$$
$$t_p = \frac{r_p^A - r_0^A}{c} = \frac{\sqrt{(pd - r\cos\theta)^2 + (l - r\sin\theta)^2} - \sqrt{r^2 + l^2 - 2rl\sin\theta}}{c} \tag{2}$$

where r_p^A denotes the distance between the damage and PZT A_p.

MUSIC algorithm preforms eigenvalue decomposition of the covariance matrix of array signals $\boldsymbol{X}(t)$ to obtain the signal and noise subspaces, and the location of signal source can be estimated based on the orthogonality between these two subspaces [15]. To describe the orthogonality between the signal subspace and noise subspace, the spatial spectrum is calculated by Eq. (3):

$$P_{MUSIC}(r,\theta) = \frac{1}{A^H(r,\theta)U_N U_N^H A(r,\theta)} \tag{3}$$

$\boldsymbol{U}_N$ denotes the noise subspace spanned by the eigenvectors corresponding to remaining small eigenvalues. By varying r and θ to realize a scanning process, $\boldsymbol{A}(r,\theta)$ is steered to scan the monitoring area. According to Eq. (3), the spatial spectrum of the whole monitoring area is obtained. When the scanning position matches the damage location,

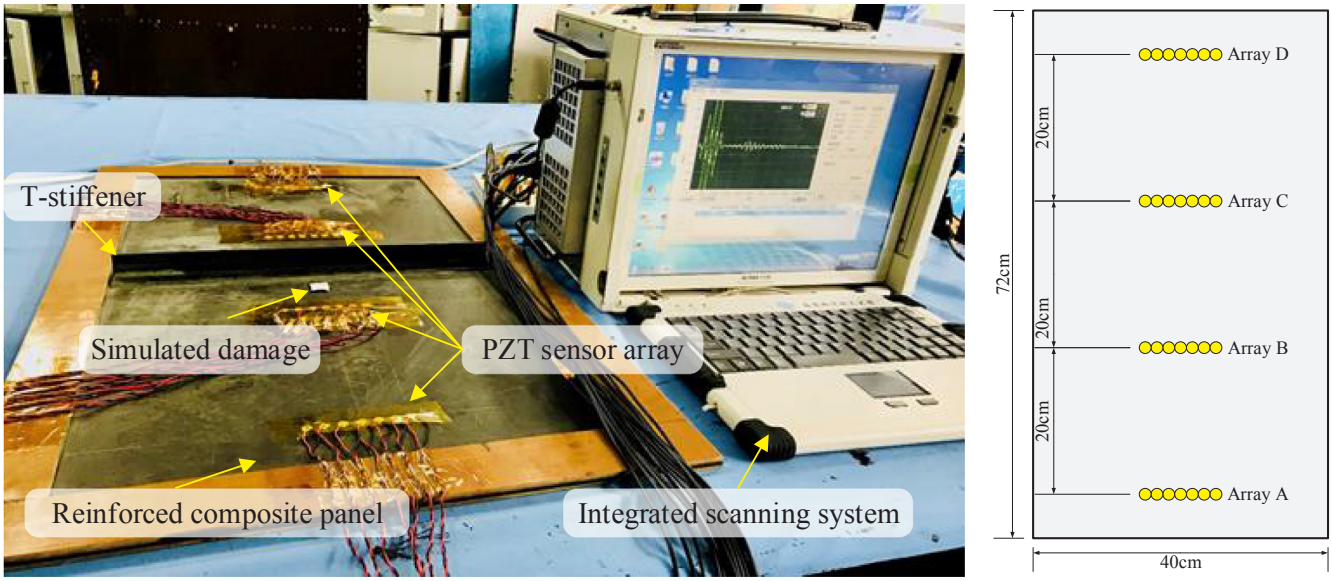

Fig. 2. The reinforced composite panel and the sensor layout.

the damage scattered signal is enhanced and the signal subspace is orthogonal with the noise subspace at the same time. Hence, the denominator of Eq. (3) approaches 0, resulting in a peak in the spatial spectrum corresponding to the damage location. Both the distance and angle of damage can be obtained as Eq. (4).

$$(\hat{r}, \hat{\theta}) = \arg\max P_{\mathrm{MUSIC}}(r, \theta) \tag{4}$$

3. Guided wave performance research on the composite structure

The guided wave performance on the composite structure is researched, including the characteristics of propagation anisotropy and propagation attenuation.

3.1. Reinforced composite panel and the experimental setup

Experimental setup includes an integrated scanning system developed by the authors' group and a reinforced composite panel with a T-stiffener, shown in Fig. 2. The integrated scanning system is utilized to generate excitation signal and acquire response signals output from the PZT sensors [31]. During the experiment, 5 cycle modified sine wave is used as the excitation signal with the amplitude of ± 70 V. Its central frequency is set to be 50 kHz to generate A0 mode dominated guided wave and its frequency band is from 40 kHz to 60 kHz. The sampling rate is set to be 10MSPS. The size of aircraft reinforced composite panel is 72 cm × 40 cm × 0.3 cm (Length × Width × Thickness), which is made of carbon fibers and has one T-stiffener in the middle. The panel has 18 stacked layers and the thickness of each layer is 0.125 mm. The ply sequence is [45/0/−45/90/0/−45/0/−45/0]s.

Four linear sensor arrays are bonded on the panel, which are named as array A, array B, array C and array D. Every array has 7 elements and the element spacing is 1.3 cm. The vertical distance between every two adjacent arrays is 20 cm. These four sensor arrays divide the panel into three monitoring areas. Among them, there exist a T-stiffener between array B and array C.

3.2. Propagation attenuation and anisotropy of guided wave

The guided wave performance on the reinforced composite panel is studied. According to the propagation path of guided wave crosses the T-stiffener or not, the signals of 6 propagation paths along different directions are analyzed, shown as Fig. 3. Among them, PZT B_{-3}-PZT A_3, PZT B_0-PZT A_0 and PZT B_3-PZT A_{-3} are 3 propagation paths which do not cross the T-stiffener, corresponding to 111°, 90° and 69° respectively. PZT C_{-3}-PZT B_3, PZT C_0-PZT B_0 and PZT C_3-PZT B_{-3} are 3 propagation paths which cross a T-stiffener, corresponding to 111°, 90° and 69° respectively. Fig. 3 also shows the signal waveforms corresponding to PZT B_3-PZT A_{-3} and PZT C_3-PZT B_{-3} respectively. The amplitude of A_0 mode corresponding to PZT B_3-PZT A_{-3} is 1.8 V and the other is 0.8 V. From the signals, the propagation velocities of these two paths are measured using the peak detection method, i.e. 1473.6 m/s and 1422.0 m/s.

Table 1 lists the amplitudes and velocities of the whole 6 propagation paths. It can be obtained the T-stiffener during the propagation of guided wave makes the attenuation more serious. The velocities along different directions also vary seriously. When the propagation path do not cross any T-stiffener, the maximum velocity error is 44 m/s. Similarly, when the propagation path crosses a T-stiffener, the maximum velocity error is 129.2 m/s. In the following section, the mean propagation velocity of guided wave is set in MUSIC algorithm, i.e. 1478.2 m/s. From Table 1, it can be seen that the composite structure makes the guided wave propagation anisotropic. And the T-stiffener increases the velocity error of guided wave along different directions, as well as the attenuation severity.

4. Synthesis aperture-MUSIC algorithm with sensor phase errors estimation

The sensor phase errors of a linear PZT sensor array caused by structural anisotropy and sensor position errors are quantitatively analyzed in this section for actuating and receiving guided waves, as well as the influence of phase errors on the localization precision of synthesis aperture-MUSIC algorithm. At last, an omnidirectional sensor phase errors estimation method is presented.

4.1. Time delay error analysis of the linear array

In practical applications, there exists the time delay error during synthesis aperture and steering vectors. Back to Eq. (1), if the practical time delay from the damage position to the q^{th} element in the sensor array is $\hat{\tau}_q$, the sensor phase error of steering vectors is defined as [25]

$$\begin{aligned}\Gamma^{S}(\theta) &= \mathrm{diag}\{e^{j\omega_0(\hat{\tau}_{-M}-\tau_{-M})} \ \cdots \ e^{j\omega_0(\hat{\tau}_q-\tau_q)} \ \cdots \ e^{j\omega_0(\hat{\tau}_M-\tau_M)}\} \\ &= \mathrm{diag}\{e^{j\omega_0\Delta\tau_{-M}} \ \cdots \ e^{j\omega_0\Delta\tau_q} \ \cdots \ e^{j\omega_0\Delta\tau_M}\}\end{aligned} \tag{5}$$

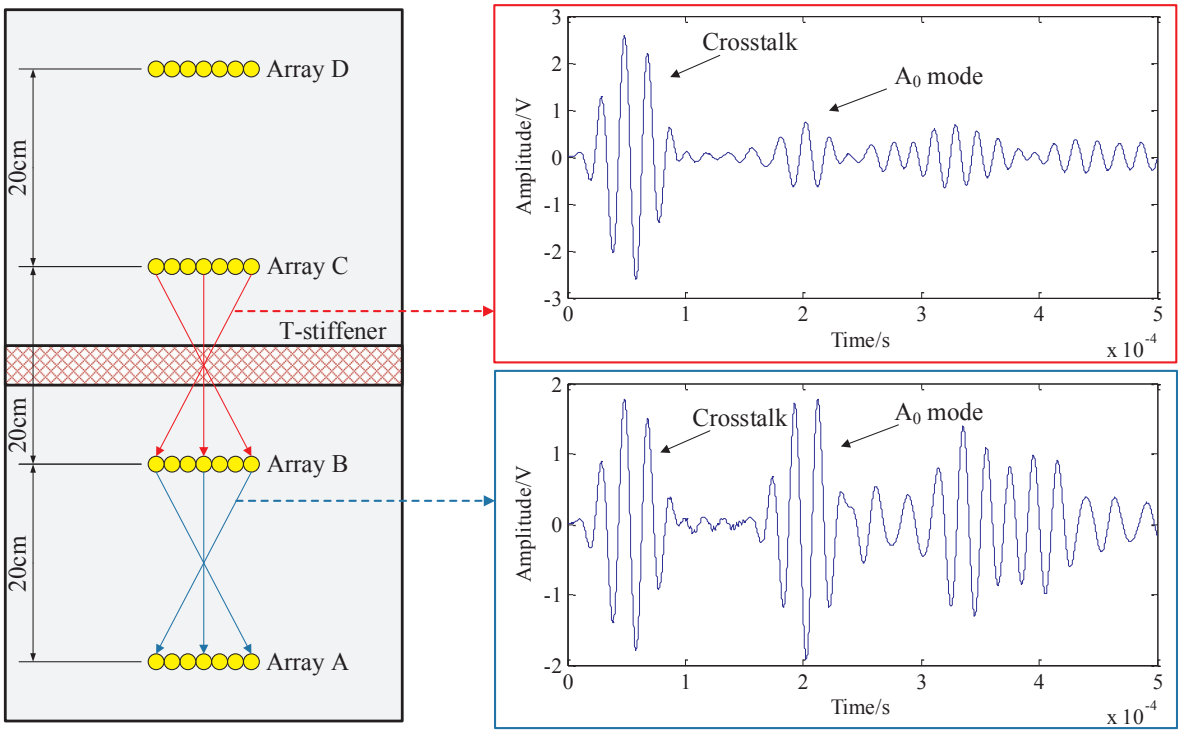

Fig. 3. Typical signal waveforms on the reinforced composite panel.

Table 1
Amplitudes and velocities of the 6 propagation paths.

Propagation paths		Amplitude	Velocity
Not cross any T-stiffener	PZT B_{-3}-PZT A_3	1.8 V	1473.6 m/s
	PZT B_0-PZT A_0	2.4 V	1429.6 m/s
	PZT B_3-PZT A_{-3}	1.9 V	1445.9 m/s
Cross a T-stiffener	PZT C_{-3}-PZT B_3	0.8 V	1422.0 m/s
	PZT C_0-PZT B_0	0.7 V	1546.8 m/s
	PZT C_3-PZT B_{-3}	0.7 V	1551.2 m/s

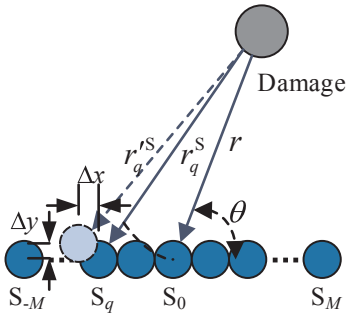

Fig. 4. Sensor position error of qth element in the sensor array.

where diag{} represents constructing the diagonal matrix with the elements in {}. Similarly, back to Eq. (2), if the practical time delay from the p^{th} element in the actuator array to the damage position is $\hat{\tau}_p$, the phase error during synthesis aperture is defined as

$$\begin{aligned}\Gamma^A(\theta) &= diag\{e^{j\omega_0(\hat{\tau}_{-M}-\tau_{-M})} \ \cdots \ e^{j\omega_0(\hat{\tau}_p-\tau_p)} \ \cdots \ e^{j\omega_0(\hat{\tau}_M-\tau_M)}\} \\ &= diag\{e^{j\omega_0\Delta\tau_{-M}} \ \cdots \ e^{j\omega_0\Delta\tau_p} \ \cdots \ e^{j\omega_0\Delta\tau_M}\}\end{aligned} \tag{6}$$

In line with Eq. (5) and (6), to estimate the sensor phase error is to obtain the time delay error $\Delta\tau_q$ and $\Delta\tau_p$ corresponding to the sensor array and actuator array respectively. In the linear PZT sensor based guided wave methods, the structural anisotropy and sensor position error are involved as general sources of the time delay error. Taking the time delay error of steering vectors for example, the following section quantitatively analyzes the influence of foregoing factors to the time delay error of each element.

(a) Time delay error caused by the structural anisotropy

The propagation velocities of guided wave vary with directions due to the anisotropy of composite structures. Given that the practical velocity from one direction is c', the time delay error $\Delta\tau_q$ is expressed as:

$$\Delta\tau_q = \frac{r_q^S}{c'} - \frac{r_q^S}{c} \tag{7}$$

If the distance between the damage to the sensor array is 20 cm, the corresponding time delay error could be calculated, where c is set identical to the measured velocity on the composite structure to be introduced in Section 3.2, i.e. 1478.2 m/s. According to Eq. (7), the corresponding time delay error would reach to $\pm\ 40 \times 10^{-7}$ s for the velocity error of ± 50 m/s.

(b) Time delay error caused by sensor position error

The sensor position error usually appears when the sensor array is being arranged on structures. As presented in Fig. 4, the position error of qth element in the sensor array is $(\Delta x, \Delta y)$. Given this, the actual distance from damage to the qth element is expressed as

$$r_q'^S \sqrt{[r\cos\theta - (id + \Delta x)]^2 + (r\sin\theta - \Delta y)^2} \tag{8}$$

The corresponding error of the time delay $\Delta\tau_q$ is defined as:

$$\begin{aligned}\Delta\tau_q &= \frac{r_q'^S - r_q^S}{c} \\ &= \frac{\sqrt{[r\cos\theta - (qd + \Delta x)]^2 + (r\sin\theta - \Delta y)^2} - \sqrt{r^2 + q^2d^2 - 2rqd\cos\theta}}{c}\end{aligned} \tag{9}$$

Following Eq. (9), time delay error caused by sensor position error is

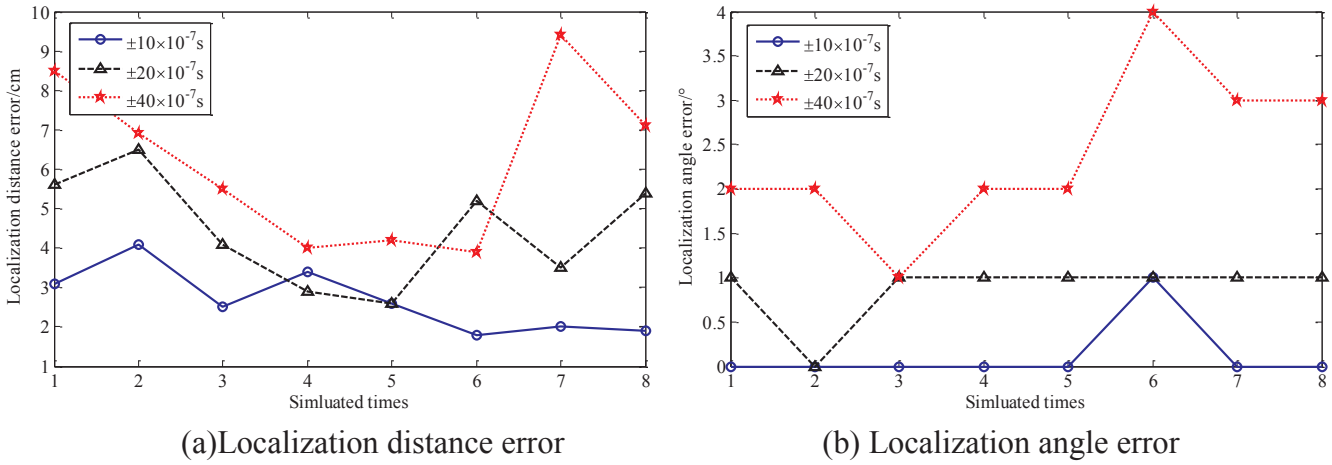

(a)Localization distance error (b) Localization angle error

Fig. 5. Localization error of MUSIC algorithm with the phase error of different severities.

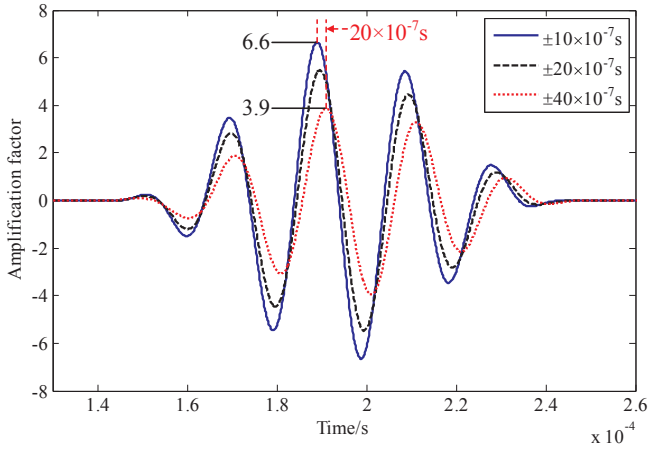

Fig. 6. Focused signal using synthesis aperture with sensor phase errors of different severities.

also concerned with the damage position and the sensor position error. Assume that the damage appears at (20 cm, 90°), the time delay error can be calculated given $q = 1$ and $d = 1.3$ cm. In this case, the time delay error reaches $\pm 10 \times 10^{-7}$ s for the sensor position error as ± 0.1 cm, respectively at X axis and Y axis.

4.2. Synthesis aperture-MUSIC algorithm precision analysis in the presence of sensor phase errors

To analyze the influence of sensor phase errors on the localization error of MUSIC algorithm, some array signals with the phase error of different severities are simulated in this section. If the damage appears at (r, θ), the time delay from damage to every element in the sensor array could be calculated via Eq. (1). On that basis, the error within certain limits is brought to the time delay of every element. The time delay with error is adopted in the normal 5-cycle modified sine waves, thus a set of array signals is established, which counts as the scattered array signal from the damage at (r, θ). To localize damage adopting the simulated array signals with MUSIC algorithm, the impact of time delay error on the MUSIC localization error is evaluated.

Assume that the damage position is (20 cm, 90°) and the time delay error are $\pm 10 \times 10^{-7}$ s, $\pm 20 \times 10^{-7}$ s and $\pm 40 \times 10^{-7}$ s, respectively. The corresponding localization error of MUSIC algorithm is presented in Fig. 5. As time delay error increases, the localization precision also decreases. When the time delay error ranges from $\pm 40 \times 10^{-7}$ s, the mean localization distance error of MUSIC algorithm is up to 7.1 cm and the mean localization angle error reaches 2.7°. Back to Section 3.1, the time delay error in practical application is larger than $\pm 40 \times 10^{-7}$ s. Given this, a sensor phase errors estimation method is critical to improve the precision and reliability of MUSIC algorithm for damage localization on composite structures.

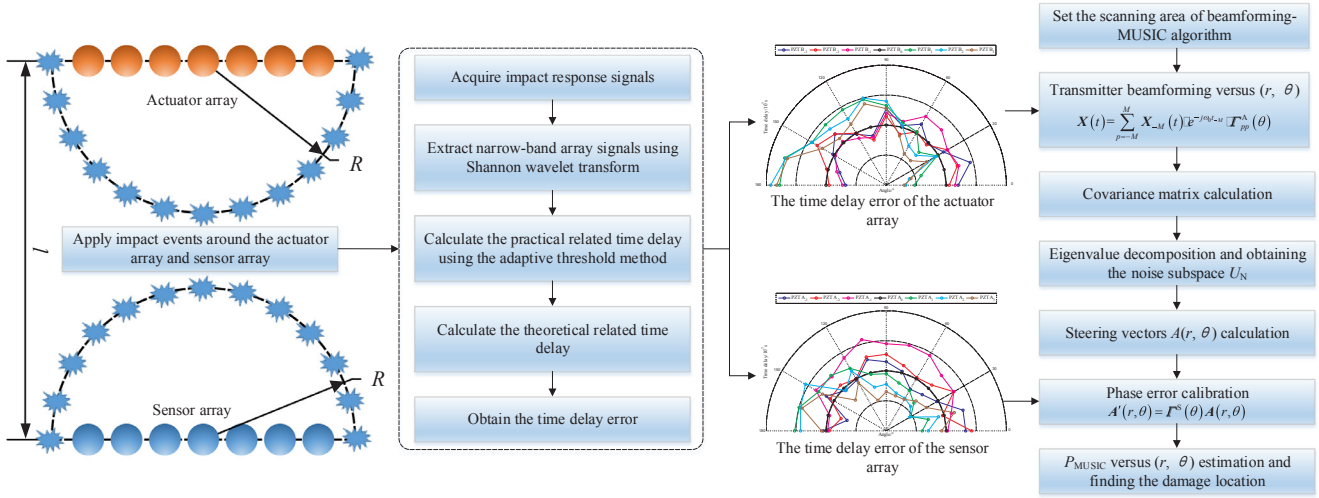

Fig. 7. Schematic diagram of synthesis aperture-MUSIC algorithm with sensor phase errors estimation.

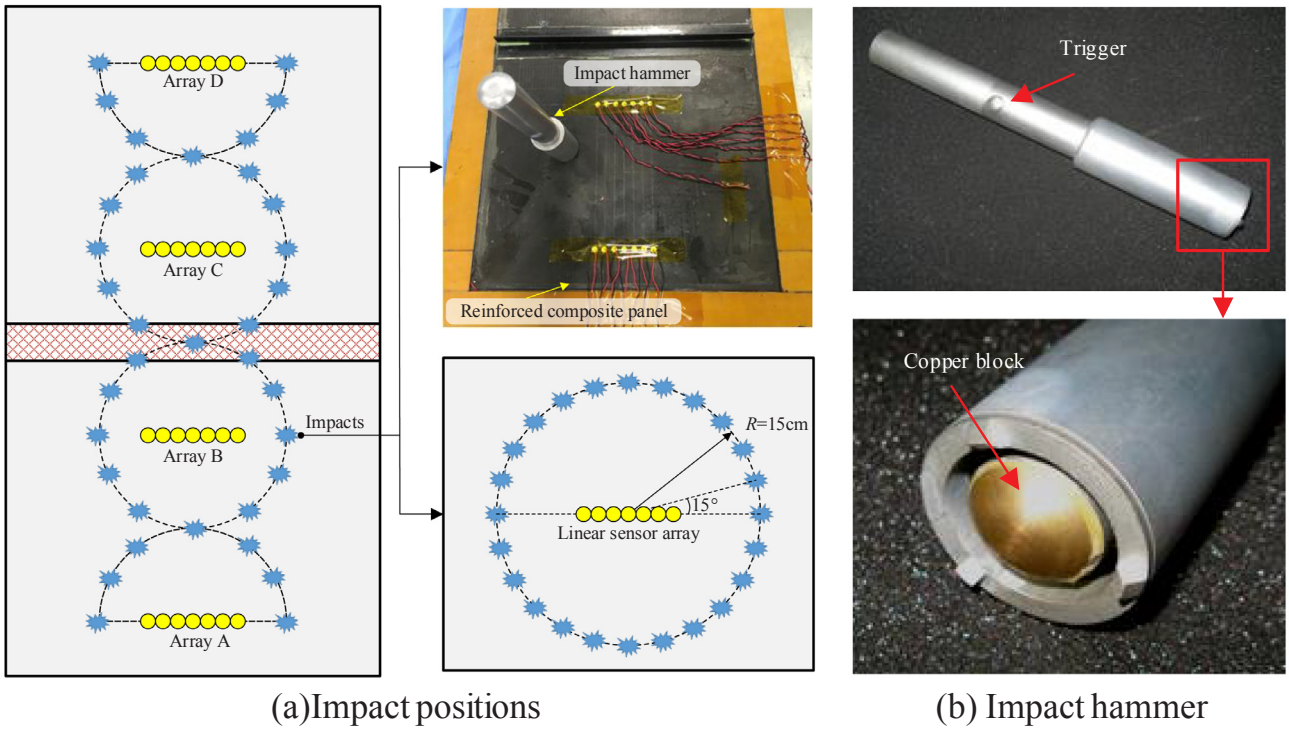

Fig. 8. Experimental setup to estimate the time delay error.

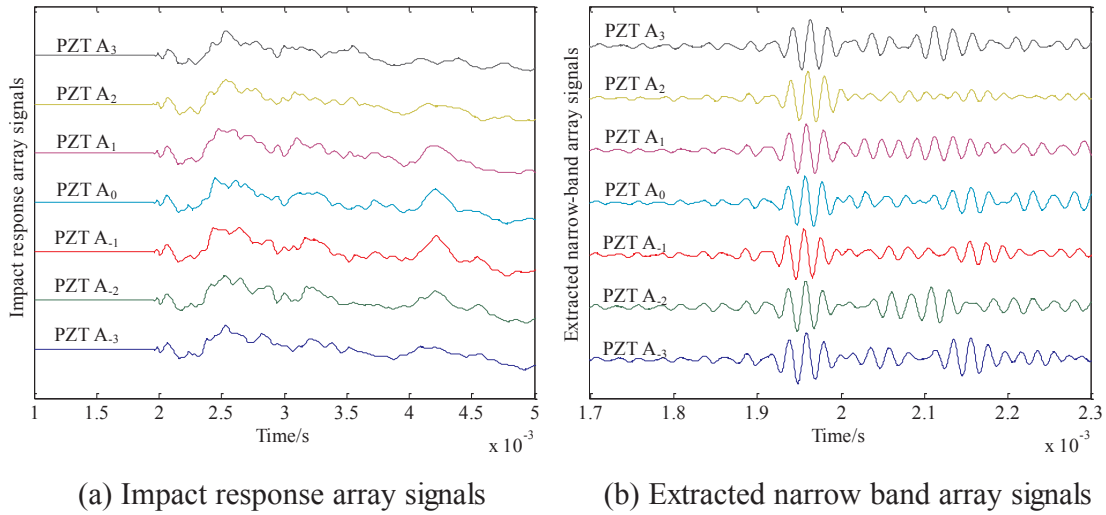

Fig. 9. Typical array signals for the time delay error estimation.

Table 2
Time delay error estimation of array A along 90°.

Time delay	PZT A_{-3}	PZT A_{-2}	PZT A_{-1}	PZT A_0	PZT A_1	PZT A_2	PZT A_3
Practical related time delay/10^{-7} s	−20	−10	0	0	20	30	40
Theoretical related time delay/10^{-7} s	36	16	4	0	4	16	36
Time delay error/10^{-7} s	−56	−26	−4	0	16	14	14

The influence of time delay error on the synthesis aperture performance is also evaluated. Fig. 6 shows the corresponding focused signals using synthesis aperture with the time delay error of ± 10 × 10^{-7} s, ± 20 × 10^{-7} s and ± 40 × 10^{-7} s respectively. It can be observed that the amplification factor of synthesis aperture would decrease with the increase of time delay error. Not only that, there exist time delay error between these focused signals. In this case, synthesis aperture signal processing cannot enhance the damage scattered signal and improve the SNR. Even worse, it also introduces additional time delay error. To compensate the phase error in synthesis aperture is also very necessary to improve the enhancement of focused signals and reduce the corresponding time delay error.

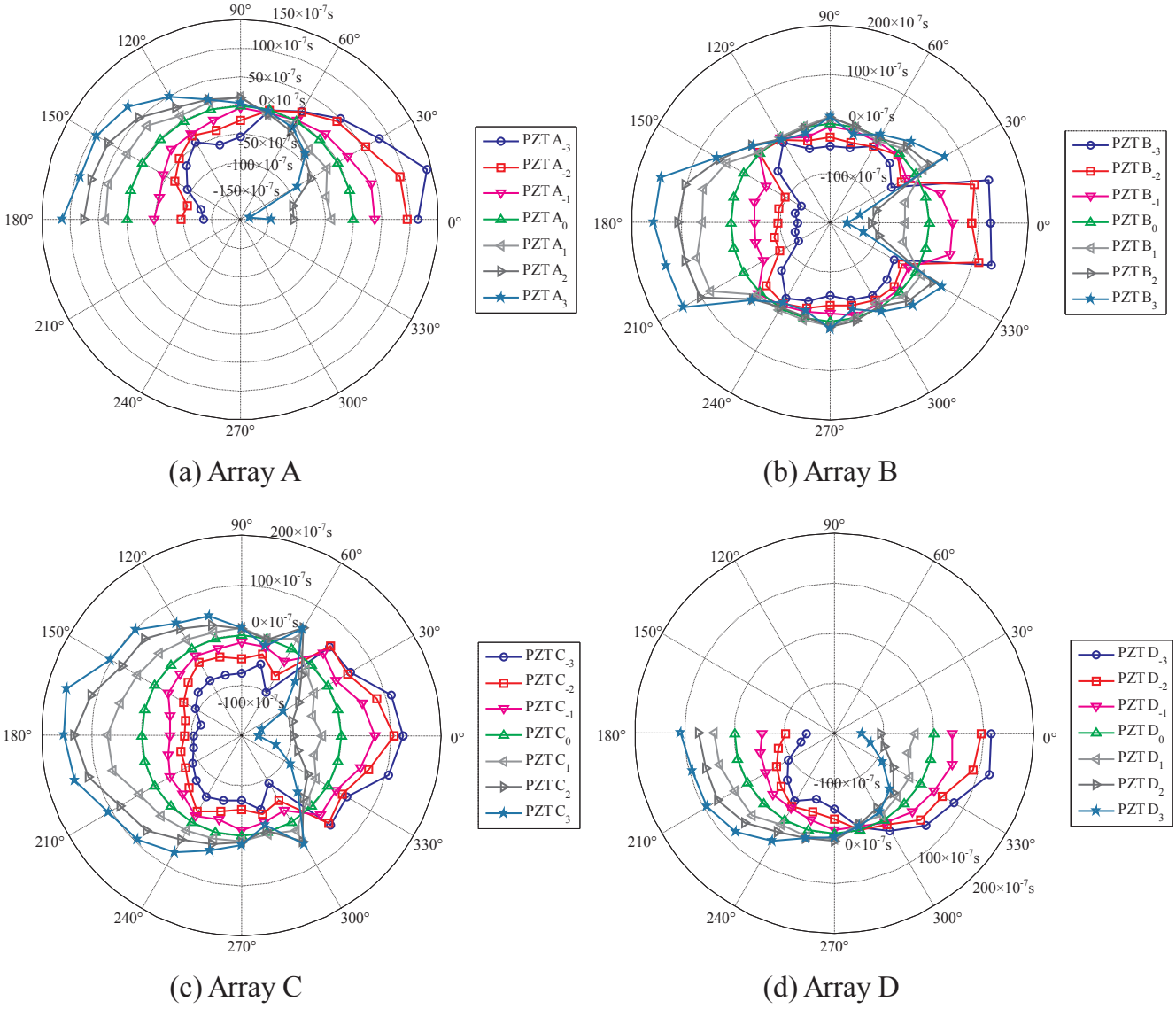

Fig. 10. Time delay error estimation results.

4.3. Sensor phase errors estimation for synthesis aperture-MUSIC algorithm

Several array error calibration techniques for compensating the sensor phase errors have aroused broad concerns in the last decades, which have been applied in radar, sonar, communication areas [26–28]. Traditional array calibration methods are classified into the active calibration methods and self-calibration methods. The self-calibration methods are deficient normally in low accuracy, high computational complexity and serious ambiguity. The active calibration methods, compared with self-calibration methods, overcome sub-optimal convergence problems with auxiliary sources and have the potential to make calibration more accurate [29]. Yet these methods require discrete auxiliary sources at known positions apart from the sensor array, which is not suitable for practical complex structures. An omnidirectional sensor phase errors estimation method is presented here, which considers the impact events at known positions as the auxiliary sources to avoid bonding additional PZT sensors on structures. On that basis, the practical time delay can be estimated by extracting the narrow band signal from the impact response array signals, which has the same center frequency in active guided wave excitation. Eventually, the phase errors are estimated through comparing the practical time delay with the theoretical time delay calculated in Eqs. (5) and (6). The flow diagram of sensor phase errors estimation for synthesis aperture-MUSIC algorithm is illustrated in Fig. 7.

This method is elucidated below. Take the sensor phase errors estimation of the sensor array for example. To simulate the auxiliary source, an impact event at the known direction θ is adopted in the structure. The impact response array signals received by the sensor array are acquired. Given that the guided wave is frequency dispersive, and impact response signals are broad band, the narrow band signal with the identical center frequency excited by active guided wave method needs to be extracted. Narrow band array signals are extracted here from impact response signals with Shannon wavelet transform [30].

After obtaining the narrow band array signals, the practical time delay from the impact to every element in the sensor array is obtained, denoted as $\hat{\tau}_q$. Given the unknown response signal at the impact position, the practical related time delay corresponding to the reference element is then calculated

$$\hat{\tau}_q^R = \hat{\tau}_q - \hat{\tau}_0, \quad q = -M, \cdots M \tag{10}$$

In accordance with Eq. (1), the theoretical time delay has been calculated as τ_q. Similarly, the theoretical related time delay is attained,

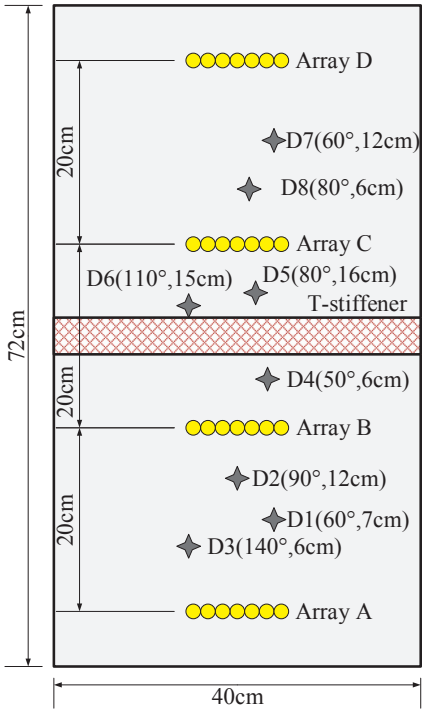

Fig. 11. Damage positions on the reinforced composite panel.

i.e. $\tau_q^R = \tau_q - \tau_0$. Accordingly, the theoretical related time delay is subtracted from the practical related time delay, and the time delay error of the sensor array along direction θ is attained.

$$\Delta\tau_q(\theta) = \hat{\tau}_q^R - \tau_q^R \tag{11}$$

Generally, the time delay error of every direction can be estimated through applying impact events from 0° to 180° around the sensor array. Once the time delay error is obtained, the phase error of the sensor array can be calculated.

$$\boldsymbol{\Gamma}^S(\theta) = \mathrm{diag}\{e^{j\omega_0\Delta\tau_{-M}} \ \cdots \ e^{j\omega_0\Delta\tau_q} \ \cdots \ e^{j\omega_0\Delta\tau_M}\} \tag{12}$$

Given the measured phase error, the steering vector could be compensated for,

$$\boldsymbol{A}'(r,\theta) = \boldsymbol{\Gamma}^S(\theta)\boldsymbol{A}(r,\theta) \tag{13}$$

Using the same method, the sensor phase error of the actuator array is also measured, denoted as $\boldsymbol{\Gamma}^A(\theta)$. Then the focused signal after sensor phase errors estimation based synthesis aperture is expressed as

$$\boldsymbol{X}(t) = \sum_{p=-M}^{M} \boldsymbol{X}_p(t)e^{-j\omega_0 t_p}\cdot\boldsymbol{\Gamma}_{pp}^A(\theta) \tag{14}$$

To simplify the phase errors estimation process while ensuring the accuracy, merely the phase errors are estimated along major directions. Assume that the phase error along one direction θ' is measured, and the measurement direction interval is$\Delta\theta$. In the search of MUSIC algorithm, when the search direction ranges from $\left[\theta' - \frac{1}{2}\Delta\theta, \theta' + \frac{1}{2}\Delta\theta\right]$, the corresponding phase error $\boldsymbol{\Gamma}^S(\theta')$ would be selected to compensate the steering vector via Eq. (13). Also, $\boldsymbol{\Gamma}^A(\theta')$ is selected to compensate for synthesis aperture via Eq. (14). The set of measurement direction interval $\Delta\theta$ depends on the severity of structural anisotropy. If the wave velocities vary seriously with the propagation directions, the measurement direction interval $\Delta\theta$ must be set as small as possible.

5. Damage localization on a reinforced composite panel

In this section, the proposed synthesis aperture-MUSIC algorithm with sensor phase errors estimation is evaluated on a reinforced composite panel to localize damages, which has been introduced in Section 3.1.

5.1. Sensor phase errors estimation

To measure the time delay error of the PZT sensor array, the integrated scanning system works at the passive monitoring mode to acquire the impact response signals. In this work mode, the sampling rate is set to be 10MSPS and the sampling points is 20000. In addition, an impact hammer is used to apply the impact on the structure, and Fig. 8(a) gives the impact positions. The impact hammer mainly consists of a trigger, an inside spring and a copper block connected to it, shown as Fig. 8(b). The mass and diameter of the copper block is 25 g and 20 mm, respectively. Compress and lock the spring by pushing the copper block, and then place the impact hammer on the structure vertically. The impact can be applied by pressing the trigger and ejecting the copper block to hit the structure.

During the measurement, 13 impacts are applied around the sensor array from 0° to 180° with the interval of 15°. The distance between impacts and the sensor array is 15 cm. Take the time delay error measurement of array A from 90° for example. Fig. 9(a) shows the impact response array signals, and the frequency content is mainly less than the

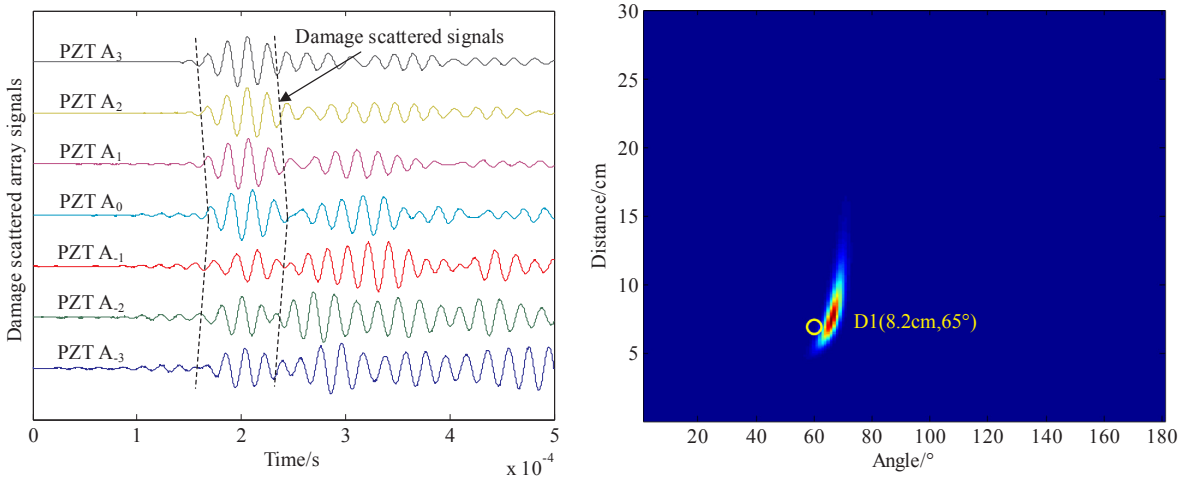

(a) Scattered array signal from D1 (b) spatial spectrum

Fig. 12. Localization result of D1 using original synthesis aperture-MUSIC algorithm.

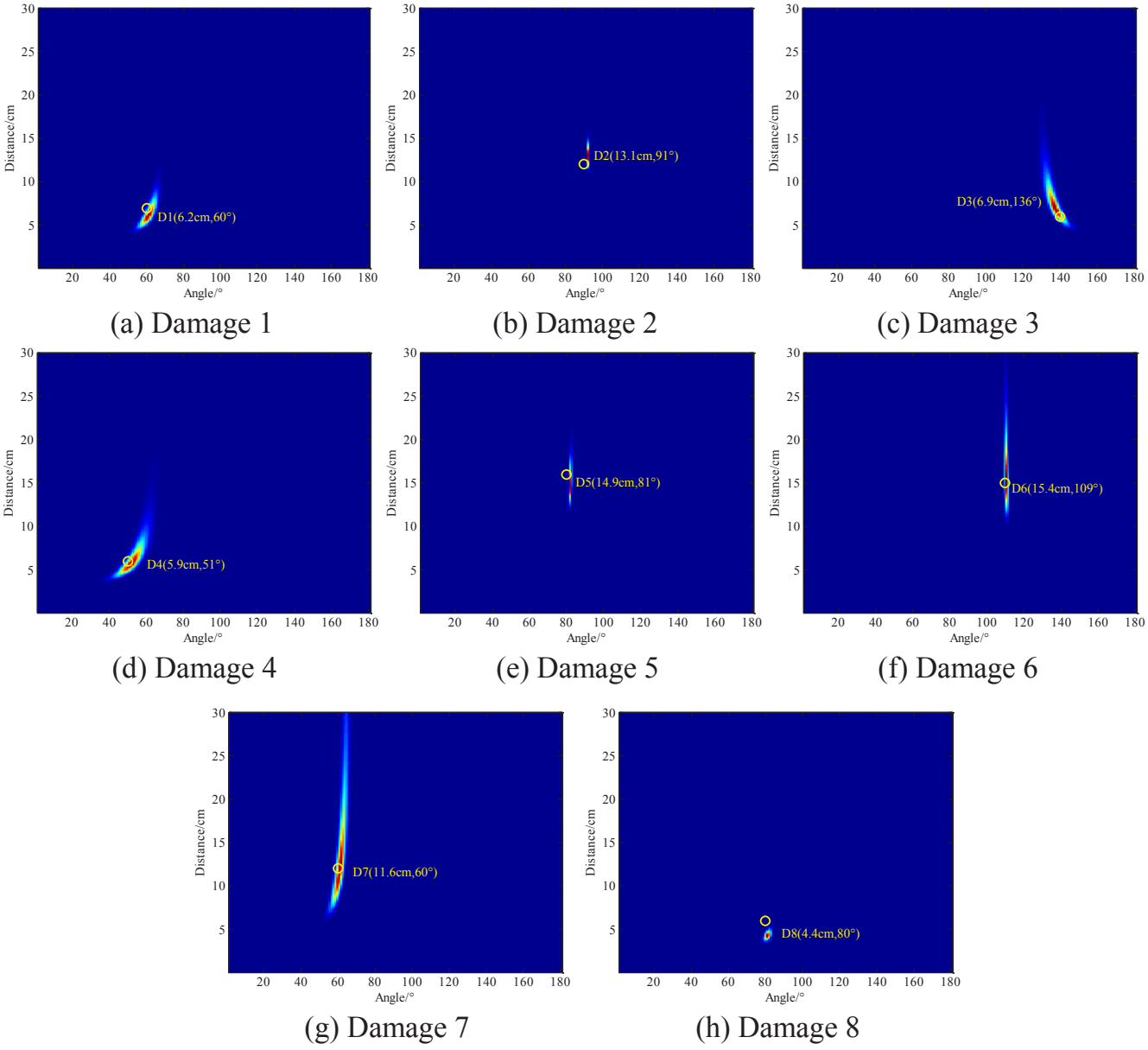

Fig. 13. Spatial spectrums of 8 damages using the proposed MUSIC algorithm.

Table 3
Localization results of 8 damages.

Damage	Locations	Original MUSIC algorithm			Anisotropy compensated MUSIC algorithm		
		Localization results	Error		Localization results	Error	
			angle	distance		angle	distance
D1	(60°, 7 cm)	(65°,8.2 cm)	5°	1.2 cm	(60°, 6.2 cm)	0°	0.8 cm
D2	(90°, 12 cm)	(97°, 11.4 cm)	7°	0.6 cm	(91°, 13.1 cm)	1°	0.8 cm
D3	(140°, 6 cm)	(158°, 4.3 cm)	18°	1.7 cm	(138°, 6.9 cm)	2°	0.9 cm
D4	(50°, 6 cm)	(61°, 6.5 cm)	11°	0.5 cm	(51°, 5.9 cm)	1°	0.9 cm
D5	(80°, 16 cm)	(87°, 18 cm)	7°	2 cm	(81°, 14.9 cm)	1°	1.1 cm
D6	(110°, 15 cm)	(107°, 11.3 cm)	3°	3.7 cm	(109°, 15.4 cm)	1°	0.4 cm
D7	(60°, 12 cm)	(62°, 10.9 cm)	2°	1.1 cm	(60°, 11.6 cm)	0°	0.4 cm
D8	(80°, 6 cm)	(86°, 4.4 cm)	6°	1.6 cm	(80°, 4.4 cm)	0°	1.6 cm

100 kHz. Then the extracted narrow band array signals with the center frequency of 50 kHz are obtained though Shannon wavelet transform, shown as Fig. 9(b). For consistency of the frequency content, the frequency band of Shannon wavelet are set from 40 kHz to 60 kHz, which is same as that of the excitation signal during damage monitoring.

After measuring the time delay of every element according to the extracted narrow band array signals, the practical related time delay corresponding to the reference element could be obtained, i.e.

-20×10^{-7} s, -10×10^{-7} s, 0×10^{-7} s, 0×10^{-7} s, 20×10^{-7} s, 30×10^{-7} s and 40×10^{-7} s respectively. Since PZT A_0 is the reference element, the time delay error of PZT A_0 is 0. Also, the theoretical related time delay can be calculated by Eq. (3), i.e. 36×10^{-7} s, 16×10^{-7} s, 4×10^{-7} s, 0×10^{-7} s, 4×10^{-7} s, 16×10^{-7} s and 36×10^{-7} s respectively. At last, the time delay error of every element in the sensor array along 90° is estimated, listed in Table 2.

As the same method, the time delay error of the array A from 0° to 180° with the interval of 15° are measured, shown as Fig. 10(a). It can be obtained the time delay error would change along different directions and the range of time delay error is $\pm 150 \times 10^{-7}$ s. The time delay error of the array B and array C from 0° to 180° with the interval of 15° are also measured, shown as Fig. 10(b) and (c). The time delay error is at the range of $\pm 200 \times 10^{-7}$ s. With the measured time delay errors, the sensor phase errors of each array can be estimated.

5.2. Damage localization results

In this experiment, the mass is bonded on the structure to simulate the damage. Totally, 8 simulated damages are made to verify the effectiveness of the proposed synthesis aperture-MUSIC algorithm with sensor phase errors estimation, namely from D1 to D8, shown as Fig. 11.

When using the synthesis aperture-MUSIC algorithm, the search area is of a distance from 0 to 30 cm and the direction from 0° to 180° with a search step of 0.1 cm distance and 1° direction respectively. For monitoring the damages between array A and array B, array B is considered as the actuator array and array A is the sensor array. Similarly, to localize D4, D5 and D6, array C is considered as the actuator array and array B is the sensor array. In this case, the propagation path of damage scattered signal crosses one T-stiffener. To localize D7 and D8, array D is considered as the actuator array and array C is the sensor array.

Fig. 12(a) shows a set of typical scattered array signal from D1 when one element is used as actuator. Using original synthesis aperture-MUSIC algorithm [19], the spatial spectrum obtained is shown as Fig. 12(b) and the localization result is (65°, 8.2 cm). Comparing with the real damage location, i.e. (60°, 7 cm), the localization distance error is 1.2 cm and the localization angle error is 5°.

Then, by using synthesis aperture-MUSIC algorithm with sensor phase errors estimation, the obtained spatial spectrum is shown as Fig. 13(a). Through finding the peak of the spatial spectrum, the localization result is obtained as (6.2 cm, 60°). Comparing with the localization result by performing the original synthesis aperture -MUSIC algorithm, the localization distance error decreases from 1.2 cm to 0.8 cm, and the localization angle error decreases from 5° to 0°. Fig. 13 also shows the other spatial spectrums of damages.

The whole localization results using synthesis aperture-MUSIC algorithm with sensor phase errors estimation for 8 damages are compared with that of original synthesis aperture-MUSIC algorithm, listed in Table 3. It can be seen that the localization distance error is less than 2 cm and the localization angle error is less than 2°. The proposed method successfully improves the corrosion localization precision.

6. Conclusions

In this paper, an anisotropy compensated MUSIC algorithm, i.e. synthesis aperture-MUSIC algorithm with omnidirectional sensor phase errors estimation, is proposed to compensate for the sensor phase errors caused by the structural anisotropy and sensor position error. This method considers impact events along different directions as calibrated sources to estimate the sensor phase errors. With the estimated phase errors, synthesis aperture signal processing and steering vectors of MUSIC algorithm are compensated. After the phase error compensation, the precision and reliability of synthesis aperture-MUSIC algorithm is improved. The proposed method is verified on a reinforced composite panel, which has one T-stiffener in the middle. Experimental results show that the damage localization error is less than 2 cm and the angle error is less than 2°.

Acknowledgement

This work is supported by Key Program of National Natural Science Foundation of China (Grant No. 51635008), Jiangsu Provincial Key Research and Development Program of China (Grant No. BE2018123), Research Fund of State Key Laboratory of Mechanics and Control of Mechanical Structures (Nanjing University of Aeronautics and Astronautics) (Grant No. MCMS-0517K01) and the Priority Academic Program Development of Jiangsu Higher Education Institutions of China.

Appendix A. Supplementary data

Supplementary data to this article can be found online at https://doi.org/10.1016/j.compstruct.2019.02.036.

References

[1] Katunin A, Dragan K, Dziendzikowski M. Damage identification in aircraft composite structures: a case study using various non-destructive testing techniques. Compos Struct 2015;127:1–9.
[2] Park B, An YK, Sohn H. Visualization of hidden delamination and debonding in composites through noncontact laser ultrasonic scanning. Compos Sci Technol 2014;100(21):10–8.
[3] Diamanti K, Soutis C. Structural health monitoring techniques for aircraft composite structures. Prog Aerosp Sci 2010;46(8):342–52.
[4] Sharifkhodaei Z, Aliabadi MH. Assessment of delay-and-sum algorithms for damage detection in aluminium and composite plates. Smart Mater Struct 2014;23(23):628–34.
[5] Sante RD. Fibre optic sensors for structural health monitoring of aircraft composite structures: recent advances and applications. Sensors 2015;15(8):18666–713.
[6] Su Z, Ye L, Lu Y. Guided Lamb waves for identification of damage in composite structures: A review. J Sound Vib 2006;295(3):753–80.
[7] Baid H, Schaal C, Samajder H, Mal A. Dispersion of Lamb waves in a honeycomb composite sandwich panel. Ultrasonics 2015;56:409–16.
[8] Murat BIS, Khalili P, Fromme P. Scattering of guided waves at delaminations in composite plates. J Acoust Soc Am 2016;139(6):3044–52.
[9] Matt H, Bartoli I, Scalea FLD. Ultrasonic guided wave monitoring of composite wing skin-to-spar bonded joints in aerospace structures. J Acoust Soc Am 2005;118(4):2240–52.
[10] Bencheikh ML, Wang Y. Joint DOD-DOA estimation using combined ESPRIT-MUSIC approach in MIMO radar. Electron Lett 2010;46(15):1081–3.
[11] Santosh S, Sharma K. A review on multiple emitter location and signal parameter estimation. Int J Eng Sci 2013;2(3):276–80.
[12] Engholm M, Stepinski T. Direction of arrival estimation of Lamb waves using circular arrays. Struct Health Monit 2011;9(2):467–80.
[13] Yang HJ, Lee YJ, Lee SK. Impact source localization in plate utilizing multiple signal classification. P I Mech Eng C-J Mec 2013;227(4):703–13.
[14] Yang H, Shin TJ, Lee S. Source location in plates based on the multiple sensors array method and wavelet analysis. J Mech Sci Technol 2014;28(1):1–8.
[15] Yuan SF, Zhong YT, Qiu L, Wang ZL. Two-dimensional near-field multiple signal classification algorithm-based impact localization. J Intel Mat Syst Str 2015;26(4):400–13.
[16] Zhong YT, Yuan SF, Qiu L. Multi-impact source localisation on aircraft composite structure using uniform linear PZT sensors array. Struct Infrastruct E 2015;11(3):310–20.
[17] Yuan SF, Bao Q, Qiu L, Zhong YT. A single frequency component-based re-estimated MUSIC algorithm for impact localization on complex composite structures. Smart Mater Struct 2015;24(10):105021.
[18] Zhong YT, Yuan SF, Qiu L. Multiple damage detection on aircraft composite structures using near-field MUSIC algorithm. Sensor Actuat A Phys 2014;214:234–44.
[19] Bao Q, Yuan S, Guo F, Qiu L. Transmitter beamforming and weighted image fusion–based multiple signal classification algorithm for corrosion monitoring. Struct Health Monit 2018. https://doi.org/10.1177/1475921718764848.
[20] Bartoli I, Marzani A, Scalea FLD, Viola E. Modeling wave propagation in damped waveguides of arbitrary cross-section. J Sound Vib 2006;295(3–5):685–707.
[21] Liu ZM. Conditional Cramér-Rao lower bounds for DOA estimation and array calibration. IEEE Signal Proc Let 2014;21(3):361–4.
[22] Kintz AL, Gupta IJ. A modified music algorithm for direction of arrival estimation in the presence of antenna array manifold mismatch. IEEE T Antenn Propag 2016;64(11):4836–47.
[23] Yamaoka T, Masada S, Sato S, Hamada N. Robust direction of arrival estimation against array sensor errors using Hopfield neural network. Electr Commun Jpn 2003;86(6):19–28.

[24] Stepinski T, Engholm M. Advanced beamforming of 2D arrays for structural health monitoring using Lamb waves Sorrento, Italy 5th European Workshop on Structural Health Monitoring. 2010.
[25] Kim J, Yang HJ, Jung BW, Chun J. Blind calibration for a linear array with gain and phase error using independent component analysis. IEEE Antenn Wirel Pr 2010;9:1259–62.
[26] Wang D. Improved active calibration algorithms in the presence of channel gain/phase uncertainties and sensor mutual coupling effects. Circ Syst Signal Pr 2015;34(6):1825–68.
[27] Dai Z, Su W, Gu H, Li W. Sensor gain-phase errors estimation using disjoint sources in unknown directions. IEEE Sens J 2016;16(10):3724–30.
[28] Liao B, Wen J, Huang L, Guo C, Chan SC. Direction finding with partly calibrated uniform linear arrays in nonuniform noise. IEEE Sens J 2016;16(12):4882–90.
[29] Liao B, Chan SC. A review on direction finding in partly calibrated arrays Hong Kong, China 19th International Conference on Digital Signal Processing. 2014.
[30] Qiu L, Yuan S, Zhang X, Wang Y. A time reversal focusing based impact imaging method and its evaluation on complex composite structures. Smart Mater Struct 2011;20(10):105014.
[31] Qiu L, Yuan S. On development of a multi-channel PZT array scanning system and its evaluating application on UAV wing box. Sensor Actuat A Phys 2009;151(2):220–30.